

# Mid-IR frequency comb source spanning 4.4–5.4 $\mu\text{m}$ based on subharmonic GaAs optical parametric oscillator

K. L. Vodopyanov,<sup>1,\*</sup> E. Sorokin,<sup>2</sup> I. T. Sorokina,<sup>3</sup> and P. G. Schunemann<sup>4</sup>

<sup>1</sup>*E. L. Ginzton Laboratory, 348 via Palou, Stanford University, Stanford, California 94305, USA*

<sup>2</sup>*Institut für Photonik, TU Wien, Gusshausstrasse 27/387, 1040 Vienna, Austria*

<sup>3</sup>*Department of Physics, Norwegian University of Science and Technology, 7491 Trondheim, Norway*

<sup>4</sup>*BAE Systems, P. O. Box 868, MER15-1813, Nashua, New Hampshire 03061-0868, USA*

\*Corresponding author: vodopyan@stanford.edu

Received April 8, 2011; revised May 13, 2011; accepted May 16, 2011;  
posted May 16, 2011 (Doc. ID 145539); published June 10, 2011

Broadband mid-IR output suitable for producing 1000-nm-wide frequency combs centered at 4.9  $\mu\text{m}$  was achieved in a degenerate subharmonic optical parametric oscillator (OPO) based on 500- $\mu\text{m}$ -long Brewster-angled orientation-patterned GaAs crystal. The OPO was synchronously pumped at 182 MHz repetition rate by 100 fs pulses from a  $\text{Cr}^{2+}:\text{ZnSe}$  laser with the central wavelength of 2.45  $\mu\text{m}$  and the average power of 100 mW. © 2011 Optical Society of America

OCIS codes: 190.4975, 190.4410.

Extending the spectral range of optical frequency combs to the mid-IR “fingerprint” region where molecules have their telltale absorption features associated with ro-vibrational transitions is critical for numerous applications, including frequency standards, precision spectroscopic measurements, and trace molecular detection. With the aid of coherent Fourier transform spectroscopy using broadband frequency combs, one can access simultaneously a great variety of molecular signatures, accurately and with high sensitivity, spectral resolution, and speed [1–5].

Several methods were developed lately for extending broadband frequency combs (and more generally, supercontinuum sources) to the mid-IR. These include direct laser sources [6], sources based on supercontinuum generation in optical fibers driven by self-phase modulation [7–9], and engineered  $\chi^{(2)}$  nonlinear optical devices [10], optical rectification [11], difference-frequency generation [12–14], optical parametric oscillators (OPOs) [15,16], and amplifiers [17].

This work extends the results of two earlier works on producing broadband frequency combs in synchronously-pumped subharmonic OPOs, based on periodically poled lithium niobate—with a 780 nm femtosecond (fs) Ti:sapphire laser [18] and fs 1560 nm erbium-fiber laser [19] as a pump. In the latter case, a spectral span of 2.5–3.8  $\mu\text{m}$  was achieved. Here, we report on our first results on exploring an even longer wavelength range—with a degenerate OPO based on orientation-patterned (OP)-GaAs crystal.

OP-GaAs has excellent characteristics for mid-IR parametric frequency conversion. It has a large second-order nonlinear optical coefficient  $d_{14} = 94 \text{ pm/V}$  [20] and good mid-IR transparency with a long wavelength cutoff at 17  $\mu\text{m}$ . In addition, it has a smaller (as compared to lithium niobate) absolute value of group velocity dispersion at  $\lambda > 3 \mu\text{m}$ .

The OPO was synchronously pumped (Fig. 1) by a femtosecond  $\text{Cr}^{2+}:\text{ZnSe}$  laser with the following parameters: central wavelength 2.45  $\mu\text{m}$ , repetition rate 182 MHz, and

pulse duration  $\sim 100$  fs. The laser was mode locked using a semiconductor saturable absorber mirror [5,6] and used a sapphire plate for the second-order dispersion compensation. Compared to [5,6], we used only a 5 mm sapphire plate for dispersion compensation and higher (6%) outcoupling, enabling the output average power to increase to 200 mW. To improve the mode quality of the laser, we used a 1.6 mm diameter aperture outside the laser cavity. At the most stable configuration, the laser average power after the aperture was 120 mW, corresponding to 100 mW at the OPO input. The ring bow-tie OPO cavity was composed of a pump-coupling dielectric mirror  $M_1$  on a  $\text{CaF}_2$  substrate with high (>95%) transmission for the pump wavelength and high (>95%) reflectivity in the 4200–5300 nm range. The other three mirrors were metallic, two of which ( $M_2, M_3$ ) were gold-coated concave mirrors with the radius of curvature 50 mm, and  $M_4$  was a protected silver-coated flat mirror.

The quasi-phase-matched (QPM) OP-GaAs structure was grown at BAE Systems by a combination of molecular beam epitaxy and hydride vapor phase epitaxy [21], resulting in QPM “film” thickness of >1 mm. The sample was 500  $\mu\text{m}$  long and had the usable aperture of  $1 \times 4$  mm. Its QPM period was 92  $\mu\text{m}$ , suitable for room-temperature subharmonic generation of  $\lambda = 2.45 \mu\text{m}$ . Thus, the GaAs crystal length amounted to only  $\sim 5$  domain reversal periods. We used type 0 nonlinear interaction (all polarizations parallel to  $\langle 111 \rangle$  direction in GaAs), and the crystal was cut and polished for Brewster-angled application in such a way that, after entering the crystal at Brewster angle, all interacting beams propagate perpendicular to the inverted domain boundaries along  $\langle 011 \rangle$ .

The ring OPO cavity had an eigenmode with the calculated signal/idler beam waist ( $1/e^2$  intensity radius) of  $w = 26 \mu\text{m}$  inside the GaAs crystal. The pump laser beam was conditioned by a telescope to a diameter and wavefront curvature before mirror  $M_1$  such that, after reflecting from curved mirror  $M_2$ , its waist inside the GaAs crystal was approximately  $w = 19 \mu\text{m}$ . The astigmatism inside the cavity, caused by the Brewster-angled GaAs,

was compensated by the opposite-sign astigmatism due to oblique ( $3^\circ$ ) incidence on the curved mirrors.

The doubly resonant condition in the degenerate synchronously pumped OPO was achieved by fine tuning the cavity length with a piezo actuator attached to the mirror  $M_4$ . Without optimization of the OPO beam outcoupling (the estimated value is  $\sim 1\%$ ), the OPO produced  $\sim 10$  mW of average power centered at  $4.9 \mu\text{m}$ , which corresponds to the intracavity circulating power of  $\sim 1$  W. With the measured pump depletion of 60%, we estimated the round trip cavity loss to be  $\sim 6\%$ , including atmospheric absorption in the nonpurged OPO cavity. The OPO threshold was measured to be approximately 40 mW of average pump power. This is larger than the calculated value of 4 mW (we used GaAs effective nonlinearity of  $d_{\text{eff}} = \frac{2}{\pi} \sqrt{\frac{4}{3}} d_{14}$  [20], where  $2/\pi$  comes from QPM interaction). This difference can be explained by some unaccounted losses inside the cavity (doubly resonant OPO threshold scales as loss squared [18]), and/or nonideal pump-OPO beam overlap.

The OPO spectrum was measured by a grating monochromator with 3.5 nm resolution and a cooled (77 K) InSb detector. The spectrum (Fig. 2) had the width of 1000 nm ( $416 \text{ cm}^{-1}$ ) at the 20 db level and was strongly affected by the atmospheric absorption (Fig. 2, gray curve). In addition, the spectral width was limited by the reflectivity range of the dielectric mirror  $M_1$  (Fig. 3) and intracavity group delay dispersion (GDD): shown in Fig. 3 is the computed extra phase accumulated per round trip versus wavelength. Also shown is parametric GaAs gain curve, which is very broad and is not the limiting factor here. Overall, the spectral band obtained from theoretical considerations is in good agreement with what we observed experimentally:  $4.4\text{--}5.4 \mu\text{m}$ . Expressed in frequency units, the OPO bandwidth exceeds that of the pump by a factor of  $\sim 2$ .

As was shown both theoretically and experimentally, the output of a subharmonic OPO is phase and frequency locked to the pump laser [18,19], and its coherence properties, e.g., carrier envelope offset (CEO) frequency and its stability, are totally inherited from the latter. The subharmonic OPO source both downconverts and broadens

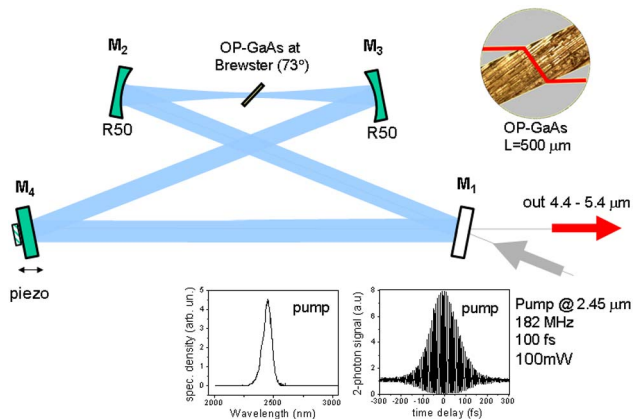


Fig. 1. (Color online) Subharmonic OP-GaAs optical parametric oscillator, synchronously pumped by fs pulses from a Cr:ZnSe ( $\lambda = 2.45 \mu\text{m}$ ) laser. Insets: side view of the OP-GaAs crystal, spectrum and second-order interferometric autocorrelation of the pump laser.

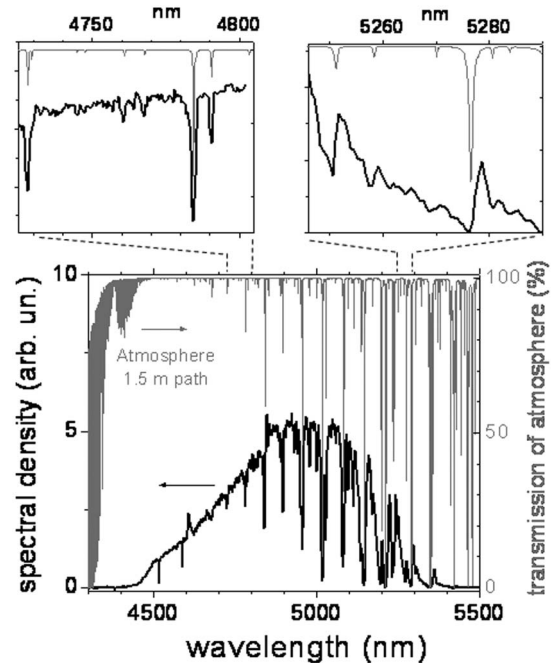


Fig. 2. OPO output spectrum measured by a grating monochromator. Atmospheric absorption peaks from HITRAN database (mostly  $\text{CO}_2$  and water vapor) corresponding to the 1.5 m path are shown in gray. Insets show zoomed shorter- and longer-wavelength wings of the OPO spectrum.

the spectrum of the pump frequency comb while preserving its coherence properties. Regarding the generated spectral density, we produce 300 nW per frequency comb tooth, which is high enough for both direct spectroscopy and phase and frequency locking to a stable cw source via beat frequency control.

Finally, we note that, while the absorption dips in the short-wavelength wing of the spectrum perfectly correlate with the absorption profile of the atmospheric water, we see asymmetric derivativelike features in the long-wavelength wing (insets in Fig. 2). In [22], the occurrence of spectral modulation of the laser output that follows the index of refraction of molecules filling the laser cavity, rather than their absorption profile, was predicted for mode-locked lasers utilizing optical soliton propagation. We suggest that the effect that we observe inside our

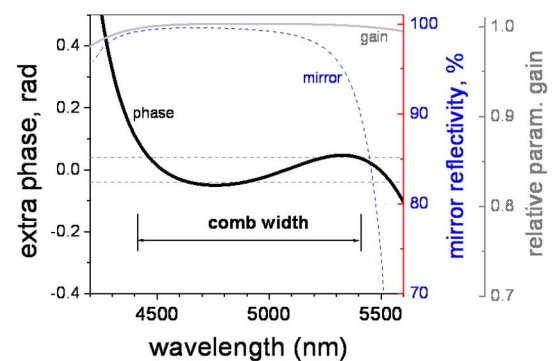


Fig. 3. (Color online) Computed extra phase accumulated per round trip due to intracavity GDD (black curve). Horizontal dotted lines indicate calculated tolerance of the OPO for extra phase. Dashed curve, reflectivity curve of the dielectric mirror; gray curve, relative parametric gain versus wavelength.

OPO cavity is of similar nature. It is only visible at longer wavelengths where the intracavity dispersion becomes anomalous (the calculated GDD of our cavity—GaAs +mirrors—becomes negative at  $\lambda > 5100$  nm). This high sensitivity to both real and imaginary parts of the refraction index may open up new opportunities for trace gas detection via intracavity spectroscopy.

In summary, we demonstrate a new mid-IR source suitable for generating a broadband frequency comb in the spectroscopically important 4.4–5.4  $\mu\text{m}$  wavelength range. By intracavity dispersion management (e.g., using chirped dielectric mirrors), purging the cavity, and increasing pump power, we expect to further broaden the instantaneous IR bandwidth. Such a source may be used for numerous applications, including broadband coherent Fourier transform spectroscopy and cavity-enhanced and dual-comb spectroscopy.

K. L. Vodopyanov wishes to thank T. Brand for fabricating GaAs crystals designed for Brewster angle operation and to acknowledge financial support from the Office of Naval Research (ONR), National Aeronautics and Space Administration (NASA), United States Air Force Office of Scientific Research (USAFOSR), Agilent Technologies, and Stanford Medical School. E. Sorokin is grateful to the Austrian Science Fund and I. T. Sorokina thanks the Research Council of Norway for financial support.

## References

1. F. Keilmann, C. Gohle, and R. Holzwarth, *Opt. Lett.* **29**, 1542 (2004).
2. K. A. Tillman, R. R. J. Maier, D. T. Reid, and E. D. McNaghten, *Appl. Phys. Lett.* **85**, 3366 (2004).
3. F. Adler, P. Masłowski, A. Foltynowicz, K. C. Cossel, T. C. Briles, I. Hartl, and J. Ye, *Opt. Express* **18**, 21861 (2010).
4. E. Sorokin, I. T. Sorokina, J. Mandon, G. Guelachvili, and N. Picqué, *Opt. Express* **15**, 16540 (2007).
5. B. Bernhardt, E. Sorokin, P. Jacquet, R. Thon, T. Becker, I. T. Sorokina, N. Picqué, and T. W. Hänsch, *Appl. Phys. B* **100**, 3 (2010).
6. I. T. Sorokina, E. Sorokin, and T. Carrig, "Femtosecond pulse generation from a SESAM mode-locked Cr:ZnSe laser," *Conference on Lasers and Electrooptics* (Optical Society of America, 2006), paper CMQ2.
7. C. L. Hagen, J. W. Walewski, and S. T. Sanders, *IEEE Photon. Technol. Lett.* **18**, 91 (2006).
8. C. Xia, M. Kumar, M.-Y. Cheng, R. S. Hegde, M. N. Islam, A. Galvanauskas, H. G. Winful, F. L. Terry, Jr., M. J. Freeman, M. Poulain, and G. Mazé, *Opt. Express* **15**, 865 (2007).
9. P. Domachuk, N. A. Wolchover, M. Cronin-Golomb, A. Wang, A. K. George, C. M. B. Cordeiro, J. C. Knight, and F. G. Omenetto, *Opt. Express* **16**, 7161 (2008).
10. C. Langrock, M. M. Fejer, I. Hartl, and M. E. Fermann, *Opt. Lett.* **32**, 2478 (2007).
11. R. A. Kaindl, M. Wurm, K. Reimann, P. Hamm, A. M. Weiner, and M. Woerner, *J. Opt. Soc. Am. B* **17**, 2086 (2000).
12. C. Erny, K. Moutzouris, J. Biegert, D. Kühlke, F. Adler, A. Leitenstorfer, and U. Keller, *Opt. Lett.* **32**, 1138 (2007).
13. A. Gambetta, R. Ramponi, and M. Marangoni, *Opt. Lett.* **33**, 2671 (2008).
14. D. Mazzotti, P. Cancio, G. Giusfredi, P. De Natale, and M. Prevedelli, *Opt. Lett.* **30**, 997 (2005).
15. J. H. Sun, B. J. S. Gale, and D. T. Reid, *Opt. Lett.* **32**, 1414 (2007).
16. F. Adler, K. C. Cossel, M. J. Thorpe, I. Hartl, M. E. Fermann, and J. Ye, *Opt. Lett.* **34**, 1330 (2009).
17. D. Brida, C. Manzoni, G. Cirimi, M. Marangoni, S. De Silvestri, and G. Cerullo, *Opt. Express* **15**, 15035 (2007).
18. S. T. Wong, K. L. Vodopyanov, and R. L. Byer, *J. Opt. Soc. Am. B* **27**, 876 (2010).
19. N. Leindecker, A. Marandi, R. L. Byer, and K. L. Vodopyanov, *Opt. Express* **19**, 6296 (2011).
20. T. Skauli, K. L. Vodopyanov, T. J. Pinguet, A. Schober, O. Levi, L. A. Eyres, M. M. Fejer, J. S. Harris, B. Gerard, L. Becouarn, and E. Lallier, *Opt. Lett.* **27**, 628 (2002).
21. C. B. Ebert, L. A. Eyres, M. M. Fejer, and J. S. Harris, *J. Cryst. Growth* **202**, 187 (1999).
22. V. L. Kalashnikov and E. Sorokin, *Phys. Rev. A* **81**, 033840 (2010).